Abstract: The singular points and asymptote lines of velocity fields are important in analyzing the properties of the fields but normally difficult to identify. We have created mesh refinement methods which can find the points and lines, and verified by analytical velocity fields. This paper briefly shows characteristics of the method for two dimensions using the two-dimensional lid-driven cavity flow.

An Application of A Mesh refinement Method Based on the Law of Mass Conservation

Zhenquan Li
School of Computing, Information and Mathematical Sciences
The University of the South Pacific
Suva, Fiji Islands
li_z@usp.ac.fj

Rajnesh Lal
School of Computing, Information and Mathematical Sciences
The University of the South Pacific
Suva, Fiji Islands
lalrajnesh@connect.com.fj

***Abstract*—The singular points and asymptote lines of velocity fields are important in analyzing the properties of the fields but normally difficult to identify. We have created mesh refinement methods which can find the points and lines, and verified by analytical velocity fields. This paper briefly shows characteristics of the method for two dimensions using the two-dimensional lid-driven cavity flow.**

Keywords-mesh refinement; mess conservation; lid-driven cavity flow; colocated finite volume method

I. INTRODUCTION

Meshing can be the process of breaking up a physical domain into smaller sub-domains (elements or cells) in order to facilitate the numerical solution of differential equations. Adaptive mesh refinement is a computational technique to improve the accuracy of numerical solutions of differential equations by starting the calculations on a coarse basic mesh (initial mesh) and then refining this mesh only there where some refinement criteria require this.

There are a large number of publications on mesh adaptive refinements and their applications. Some refinement methods use the refinement criterion which is based on local truncation errors [e.g., 1, 2, 3, 4]. The other common methods include h-refinement (e.g. [13, 16]), p-refinement (e.g. [2, 17]) or r-refinement (e.g. [14, 15]), with various combinations of these also possible (e.g. [5, 6]). The overall aim of these adaptive algorithms is to allow a balance to be obtained between accuracy and computational efficiency. The h-refinement is a method where meshes are refined and/or coarsened to achieve a prescribed accuracy and efficiency. The p-refinement is a method where method orders are assigned to elements to achieve exponential convergence rates and r-refinement is a method where elements are moved and redistributed to track evolving non-uniformities.

We have introduced adaptive mesh refinement methods in a different point of view for two-dimensional velocity fields in [12] and for three-dimensional fields in [11]. Our refinement methods are based on the law of mass conservation for two-dimensional (2D) and three-dimensional (3D) incompressible and compressible steady flows, and can be used to the problems in Fluid Engineering.

This paper shows the some results of the refinement method for 2D lid-driven cavity flow. We solve the Navier-Stokes equations with the boundary conditions numerically using a second order collocated finite volume scheme with a splitting method for time discretization in [8] and then apply the refinement method to the numerical solution once. The singular points and separation lines are identified.

II. COLOCATED FINITE VOLUME SCHEME WITH A SPLITTING METHOD FOR THE TIME DISCRETIZATION

In this section, we briefly introduce the collocated finite volume scheme given in [8].

A. Navier-Stokes equations for imcompressible fluids

For given volume force $\mathbf{f} = (f_u, f_v)$, we look for the velocity field $\mathbf{u}$ and the pressure p that satisfy

$$\frac{\partial \mathbf{u}}{\partial t} - \upsilon \Delta \mathbf{u} + (\mathbf{u} \cdot \nabla)\mathbf{u} + \nabla p = \mathbf{f} \quad \text{in } \Omega \times [0,T], \tag{1}$$

$$div\, \mathbf{u} = 0, \tag{2}$$

where $\upsilon > 0$ is the kinematic viscosity, $\mathbf{u} = (u(x,y,t), v(x,y,t))$, and $t \geq 0$. On the boundary $\partial\Omega$ of Ω, a Dirichlet no-slip boundary condition is used:

$$\mathbf{u}|_{\partial\Omega} = \mathbf{g}$$

B. Time Discretization

The time disretization for (1) and (2) used in this paper is described in Subsection 2.1 in [8].

C. Finite Volume Discretization

The finite volume discretization for (1) and (2), and the boundary implementation are given in Subsections 2.2 and 2.3 in [8].

III. CONDITIONS FOR MESH REFINEMNT

In this section, we summarize the mesh refinement method based on the law of mass conservation in [12].

Assume that $\mathbf{V}_l = \mathbf{AX} + \mathbf{B}$ is the linear interpolation of a vector field at the three vertexes in a triangle, where $\mathbf{A}$ is a 2×2 constant matrix and $\mathbf{B}$ a 2×1 constant vertical vector, and $\mathbf{X} = \begin{pmatrix} x_1 \\ x_2 \end{pmatrix}$. $\mathbf{V}_l$ is unique if the area of the triangle is not zero [13]. Mass conservation for an incompressible fluid means that

$$\nabla \cdot \mathbf{V}_l = trace(\mathbf{A}) = 0 . \qquad (4)$$

Let f be a scalar function depending only on spatial variables. We assume that $f\mathbf{V}_l$ satisfies (4) and then calculate the expressions of f. The expressions of f for the four different Jacobean forms of coefficient matrix $\mathbf{A}$ are given in Table 1 in [12]. The conditions (MC) that $f\mathbf{V}_l$ satisfies (4) in its triangle domains are the functions f in Table 1 not equaling zero or infinity in these triangular domains.

We consider quadrilateral mesh here. The algorithm which uses the conditions (MC) to refine a quadrilateral element in a given mesh is given in [12].

In this paper, we subdivide a quadrilateral by connecting the mid-points of the two opposite sides of a quadrilateral and the threshold number T=1, i.e., we subdivide an element once only.

IV. Lid-driven Cavity Flow

We show the refined meshes for two-dimensional lid-driven cavity flows for Reynolds number *Re*=1000, 2500, and 500, respectively. The approach we used in this paper for the finite volume method is that we defined the nodal locations first and then construct CVs (control volume) around them [9]. We show the comparisons of *u* and *v* profiles between the results obtained from the collocated finite volume method in Section II and the corresponding benchmark results in [7]. The benchmark results in [7] were obtained from 601×601 elements. The accuracy of the computational results from the collocated finite volume method used in this paper can be found from the comparisons. The refined meshes are based on the computational velocity fields.

A. *Re=1000*

We generated the following *u* and *v* profiles, and streamlines and refined mesh using 41×41 elements.

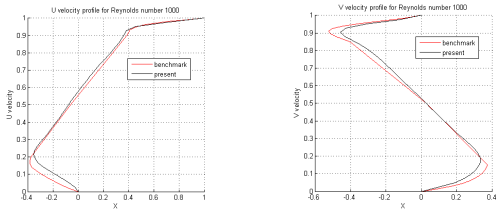

Figure 1. Comparison of *u* and *v* profiles.

In Fig. 1, *u* profile has reasonable accuracy except in the bottom-left corn; v profile also shows reasonable accuracy except at the two turning points.

Fig. 2 shows the streamlines within refined mesh. We can also see the accuracy from the streamlines, e.g., the streamline in the middle of the region should be closed streamline, but in Fig. 2 it is spiral with small increment due the law of mass conservation is not satisfied [10]. The three isolated red crosses identify the center locations for the three vortices, primary vortex, and three secondary vortices: BL1-the bottom left secondary vortex, BR1-the bottom right secondary vortex, and TL1-the top left secondary vortex. The centers of primary vertex, BR1 and BL1 vortices have been identified.

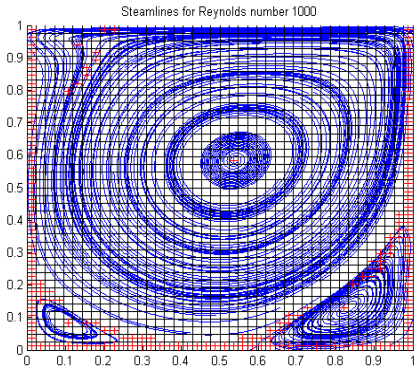

Figure 2. Streamlines within refined mesh.

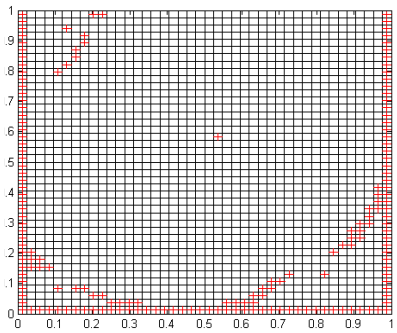

Figure 3. Refined mesh.

Fig. 3 shows the refined mesh without streamlines. The further calculations for velocity field and other unknowns will be based on this refined mesh.

B. *RE=2500*

The following *u* and *v* profiles, and streamlines and refined mesh were drawn using 69×69 elements.

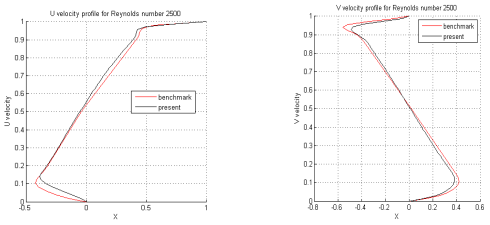

Figure 4. Comparison of *u* and *v* profles.

Fig. 4 shows the similar accuracy to Fig. 1 using finer mesh. It is normally accepted that the structure of flows becomes complicated when Reynolds number is increased.

Fig. 5 shows the streamlines within refined mesh where a top left secondary vortex is identified. A bottom left tertiary vortex and a bottom right tertiary vortex are identified in [7]. These vortices may be identified when we refine mesh further using refinement criteria given in Section III. The centers of primary vortex, BL1, BR1 and TL1 are identified.

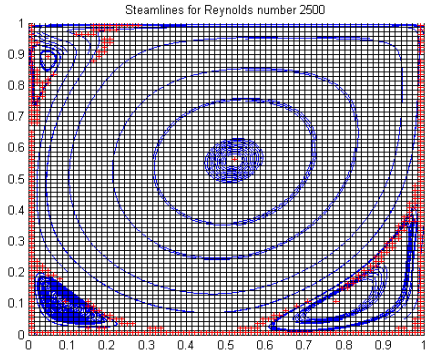

Figure 5. Streamlines with refined mesh.

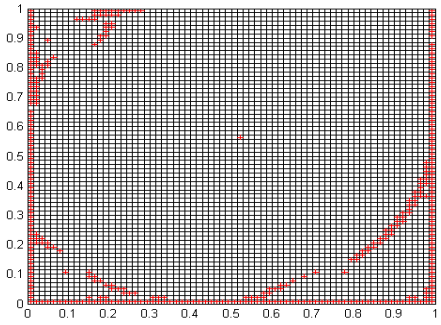

Figure 6. Refined mesh

C. *RE=5000*

We use a mesh with 79×79 elements in drawing the following *u* and *v* profiles, and streamlines.

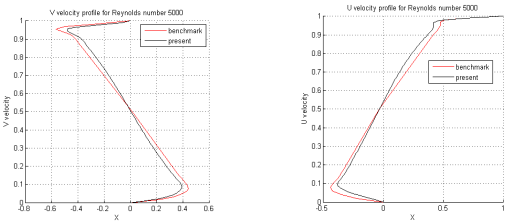

Figure 7. Comparison of *u* and *v* profiles.

Fig. 8 shows the streamlines within refined mesh. Since the streamlines are drawn not very accurately as shown in other figures, the refined mesh and the streamlines may have some difference in the separation boundaries, especially in the right bottom corner. Table 1 in the following subsection shows the accuracy of the refined mesh in identifying the vortex center locations.

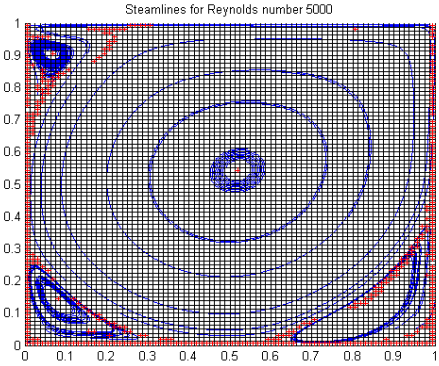

Figure 8. Streamlines within refined mesh.

In the right bottom corner, we can view the tertiary vortex but we cannot identify the center but this may be done after further refinements. We may also know from the refined mesh that the structure of the field may be complicated in the top left corner.

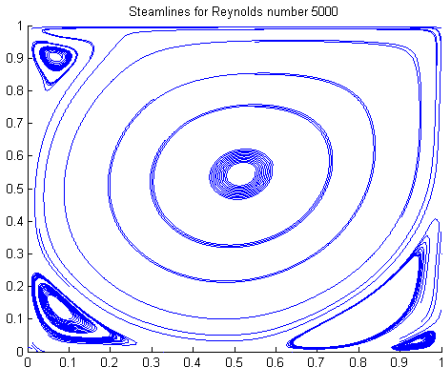

Figure 9. Streamlines.

Fig. 9 shows some streamlines drawn by different seed points using the computational velocity field calculated. The tertiary vortex in the right bottom corner is presented.

D. Vortex center locations

All centers of primary, secondary and tertiary vortices are found in [7] for *re=1000*, *2500*, and *5000*. We use much less coarse meshes than the mesh with 601×601 elements in [7] so we find the center locations of primary, and secondary vortices. Further refined meshes may show the tertiary vortices and provide more accurate center locations.

The coordinates in Table 1 are coordinates of the intersections of the isolated red crosses which can be viewed as the approximations of the center locations with an error 1/N/2 where N is the number of points inserted in the *x* and *y* intervals of the domain, for example, 1/41/2=0.012 for Re=1000. The accuracy will be improved after further refinement is implemented as we did for analytical velocity fields [12]. The locations of the centers might change slightly if further refinements have been applied.

TABLE I. PRIAMRY AND SECOND VORTEX CENTRE LOCATIONS

Vortex Type	**Reynolds numbers**		
	Re=100	***Re=2500***	***Re=5000***
Primary vortex	(0.5357, 0.5833) (0.5300, 0.5650)[a]	(0.5300, 0.5500) (0.5200, 0.5433)	(0.5188, 0.5437) (0.5150, 0.5317)
BR1	(0.8214, 0.1310) (0.8633, 0.1117)	(0.8300, 0.0900) (0.8350, 0.0917)	(0.8621, 0.0603) (0.8050, 0.0733)
BL1	(0.1070, 0.0833) (0.0833,0.0783)	(0.0982, 0.1161) (0.0950, 0.1100)	(0.0813, 0.1437) (0.0733,0.1367)
TL1	-	(0.0447, 0.8839) (0.0433, 0.8900)	(0.0688, 0.9063) (0.0633, 0.9100)

a. The coordinates in blue in this table are the results in [7]

V. DISCUSSION

This paper presents the initial results from the mesh refinement method in [12] using collocated finite volume approach introduced in [8]. From the *u* and *v* profiles in Figs. 1, 4 and 7, we may need to look at the nodal locations in [9] at the bottom boundary since some errors appear there. The further mesh refinement is our further research topic.

ACKNOWLEDGMENT

We thank Prof. Shigeyoshi Watanabe at the University of Electro-Communications, Japan for his many valuable comments.

REFERENCES

[1] A. Almgren, J. Bell, P. Colella, L. Howell, and M. Welcome, "A conservative adaptive projection method for the variable density incompressible navier-stokes equations," J. Comp. Phys., vol. 142, pp. 1-46, 1998.

[2] J. Bell, M. Berger, J. Saltzman, and M. Welcome, "Three dimensional adaptive mesh refinement for hyperbolic conservation laws," J. Sci. Comput., vol. 15(1), pp.127-138, 1994.

[3] M.J. Berger and J. Oliger, "Adaptive Mesh Refinement for Hyperbolic Partial Differential Equations," J. Comput. Phys., vol. 53, pp. 484-512, 1984.

[4] M.J. Berger and P. Colella, "Local adaptive mesh refinement for shock hydrodyamics," J. Comput. Phys., vol. 82(1), pp. 64-84, 1989.

[5] P.J. Capon and P.K. Jimack, "An Adaptive Finite Element Method for the Compressible Navier-Stokes Equations," Numerical Methods for Fluid Dynamics, Vol. 5, M.J. Baines and K.W. Morton, Eds. OUP, 1995.

[6] L. Demkowicz, J.T. Oden, W. Rachwicz and O. Hardy, "An h-p Taylor-Galerkin Finite Element Method for the Compressible Euler Equations," Comp. Meth. in Appl. Mech. and Eng., vol. 88, pp. 363-396, 1991.

[7] E. Erturk, T. C. Corke, and C. Gökcöl, "Numerical solutions of 2-D steady incompressible drven cavity flow at high Reynolds numbers," Int. J. Numer. Meth. Fluids, Vol. 48, pp. 747-774, 2005.

[8] S. Faure, J. Laminie, and R. Temam, "Colocated finite volume schemes for fluid flows", Commun. Comput. Phys, vol. 4, pp. 1-25, 2008.

[9] J. H. Ferziger, M. Peric, Computational methods for fluid dynamics. Springer, 2002.

[10] Z. Li, "A mass conservative streamline tracking method for two dimensional CFD velocity fields," Journal of Flow Visualization and Image Processing, vol. 9, pp. 75-87, 2002.

[11] Z. Li**,** "An adaptive three-dimensional mesh refinement method based on the law of mass conservation," Journal of Flow Visualization and Image Processing, vol. 8, pp. 375-395, 2007.

[12] Z. Li**,** "An adaptive two-dimensional mesh refinement method based on the law of mass conservation," Journal of Flow Visualization and Image Processing, vol. 15, pp. 17-33, 2008.

[13] R. Lohner, "An adaptive finite element scheme for transient problems in CFD," Comp. Meth. in Appl. Mech. and Eng., vol. 61, pp. 323-338, 1987.

[14] K. Miller and R. Miller, "Moving finite elements, Part I," SIAM J. on Numer. Anal., vol. 18, pp. 1019-1032, 1981.

[15] M.C. Mosher, "A variable node finite element method," J. of Comp. Phys., vol. 57, pp. 157-187, 1985.

[16] W. Speares and M. Berzins, "A 3-D Unstructured Mesh Adaptation Algorithm for Time-Dependent Shock Dominated Problems," Int. J. for Numer. Meth. in Fluids, vol. 25, pp. 81-104, 1997.

[17] O.C. Zienkiewicz, D.W. Kelly and J.P. Gago, "The hierarchical concept in finite element analysis," Int. J. of Comp. and Structures, vol. 16, pp. 53-65, 1983.